Case Studies in Construction Materials 18 (2023) e01818

Contents lists available at ScienceDirect

Case Studies in Construction Materials

journal homepage: www.elsevier.com/locate/cscm

A review of 3D printing low-carbon concrete with one-part geopolymer: Engineering, environmental and economic feasibility

Yazeed A. Al-Noaimat [a], Seyed Hamidreza Ghaffar [a,b,*,1], Mehdi Chougan [a], Mazen J. Al-Kheetan [c]

[a] Department of Civil and Environmental Engineering, Brunel University London, Uxbridge UB8 3PH, United Kingdom
[b] Applied Science Research Center, Applied Science Private University, Jordan
[c] Civil and Environmental Engineering Department, College of Engineering, Mutah University, P.O. Box 7, Mutah, Karak 61710, Jordan

ARTICLE INFO

Keywords:
3D printing
One-part geopolymers
Solid activator
Fresh properties
Hardened properties
Environmental impact
Cost assessment

ABSTRACT

3D printing is a developing technology that has the ability to use different materials to produce concrete elements with complex shapes. The utilization of geopolymers or alkali-activated materials (AAMs) in 3D printing is receiving significant interest due to the environmental benefits of replacing ordinary Portland cement (OPC). The use of solid activators to produce a one-part geopolymer can help the broader use of geopolymers at large scales, as the corrosive, viscous, and hazardous liquid activators used in two-part geopolymers do not present a feasible large-scale solution for this technology. This paper reviews the 3D printable one-part geopolymers, their compositions, and the effect of different precursor compositions, activator content, and different admixtures on the fresh and hardened properties of the mixtures. The environmental impact and cost assessment of one-part geopolymers produced by conventional and 3D printing methods are also discussed and compared to OPC and two-part geopolymers. This review concluded that one-part geopolymers are easier to mix and use than two-part geopolymers and have a lower carbon footprint than two-part geopolymers and OPC concrete. However, one-part geopolymers may not be as strong as two-part geopolymers, but they are still better than OPC.

1. Introduction

3D printing technology has been widely researched and developed in many fields [1]. 3D printing technology has enabled fully automated processes in various disciplines, including manufacturing, art, medicine, and engineering [2]. Printing concrete starts with the 3D modelling of an element or a component, followed by the deposition of layers on top of each other until completion. To avoid cold joint, the deposited material should not harden immediately. Therefore, a thixotropic material that can be smoothly extruded and hold the weight of the subsequent layers to provide shape stability is the most suitable for 3D printing applications [3–6]. Pegna announced the first successful application of 3D-printed concrete in buildings in 1997, with a series of hollow concrete structures [7]. 3D printing of concrete received significant interest in the past few years from industry practitioners and researchers due to its benefits in reducing construction time, workforce, cost, and waste materials during the removal of formwork [8,9]. It also enhances the freedom of architectural designs and the safety of conducted work compared with conventional construction approaches [9].

* Corresponding author at: Department of Civil and Environmental Engineering, Brunel University London, Uxbridge UB8 3PH, United Kingdom.
E-mail address: seyed.ghaffar@brunel.ac.uk (S.H. Ghaffar).
[1] https://orcid.org/0000-0002-4694-9508

https://doi.org/10.1016/j.cscm.2022.e01818
Received 22 October 2022; Received in revised form 7 December 2022; Accepted 29 December 2022
Available online 30 December 2022

The building industry is responsible for almost 40% of solid waste generation, 40% of energy consumption, 12% of water depletion, and 46% of anthropogenic and greenhouse gas emissions [10]. The sustainability of materials and construction processes is crucial due to the growing industrialization and large-scale construction projects planned worldwide, which will most likely increase negative environmental impacts [11]. Many researchers believe that 3D printing offers environmental benefits, reductions in costs, and efficiency over conventional concrete structures [12,13]. However, using concrete mixtures compatible with this technology requires 1.5 – 2 times more cement than conventional casting methods, which might lead to more CO_2 being released into the atmosphere [14–16]. In addition, cement is considered the most energy-intensive component of concrete. Accordingly, various studies have been conducted on using supplementary cementitious materials (SCMs) as an alternative to OPC in the 3D printing of concrete [17–19]. When using SCMs in 3D printing to partially replace PC, it is essential to consider the fresh properties of the designed mix, such as the printability and setting time [20]. Moreover, the effect of SCMs on concrete properties depends on SCMs physiochemical characteristics [21]. At an early age, incorporating SCMs reduces strength due to the dilution effect of cement. However, the strength can be increased when using a highly reactive material such as silica fume and calcined clay [22–25].

More recently, researchers have been interested in the 3D printing of alkali-activated materials (AAMs), also known as geopolymers, due to their ability to reduce the CO_2 footprint associated with traditional concrete production [26,27]. Geopolymer is a two-part mixture produced by mixing an alkaline solution with precursors composed of alumina- and/or aluminosilicate-rich materials such as fly ash and metakaolin. Most recently, a promising material called laterite was used as the precursor due to its high abundance and good performance [28]. The precursors are activated by alkaline activators such as alkali hydroxide, silicate, and aluminate [29–32]. Geopolymer has several advantages over traditional concrete, such as high compressive strength, fire resistance, rapid hardening, salt and acid resistance, and other environmental benefits [33–35]. Despite all the benefits of two-part geopolymer, some challenges regarding the viscosity and the handling of hazardous alkaline activator solutions for large-scale printing should be considered. Accordingly, using a solid activator to produce a one-part geopolymer can help solve some of the challenges [36–38]. In addition to water, only a dry combination is required to form one-part mixes, where a solid alkali-activator in powder form is combined with a solid aluminosilicate precursor.

In the last few years, several studies have been conducted to investigate the efficiency and performance of using one-part geopolymers ''just add water'' in 3D printing applications as a solution to the above-mentioned problem and results revealed encouraging performance data in various characteristics. Thus, making it a suitable material to use in industrial applications. Accordingly, this paper aims to comprehensively present the development of one-part geopolymers in 3D printing technology. Numerous review papers cover various aspects of the 3D printing of two-part geopolymers and conventional cast one-part geopolymers [38–40]. In light of the benefits of one-part geopolymers over two-part geopolymers, which include the elimination of handling, transporting and operating of the hazardous activator solution on-site and in the 3D printing process, this review has focused on different aspects of 3D printing of one-part geopolymers. To the best of the authors' knowledge, 3D printing of one-part geopolymers has not been reviewed before. This paper reviews the constituents of one-part geopolymers and highlights the most commonly used precursors and solid activators. The most common techniques utilized for 3D printing geopolymer are introduced. The effect of different mix formulations and parameters (i.e., precursor type, activator types and dosages, admixtures and additives addition) on the fresh and hardened properties of 3D-printed one-part geopolymers are discussed. The environmental and economic feasibility of one-part geopolymers and 3D printing technology is also discussed and reviewed compared to more traditional solutions.

2. 3D printable concrete mixtures

The printable mixtures for 3D printing contain a higher amount of binder and fine aggregates than conventional concrete to enhance the shape stability and yield stress [15]. The absence of coarse aggregates from the mixture decreases the segregation and blockage issues [41]. In order to facilitate pumping and extrusion, printable concrete mixes usually have low dynamic yield stress. However, after extrusion, the extruded mixture should exhibit high static yield stress to enable the concrete to support its own weight and the weight of the successive printed layers [42–45].

Geopolymers are composed of natural materials or waste products as a precursor, which is activated using alkali or acid reactions. The primary reason for using geopolymers as a construction material is to replace OPC to reduce the environmental impact of concrete. The most commonly used materials as the precursor of geopolymers are fly ash (FA), silica fume (SF), ground granulated blast furnace slag (GGBS), and metakaolin (MK) [46]. According to ASTM C-618 [47], FA is a by-product material produced from burning coal, and it is divided into two categories, depending on the chemical composition of coal, class F and class C. The chemical composition of class F should contain silicon dioxide (SiO_2), aluminum oxide (Al_2O_3), and iron oxide (Fe_2O_3), which are equal to or greater than 70% of FA chemical composition, while for class C, they should be equal to or greater than 50% of FA chemical composition [5]. SF is a fine pozzolanic by-product that results from the production of ferrosilicon or silicon alloys in electric arc furnaces, and it is composed mainly of amorphous silica [48]. In contrast, GGBS is a glassy granular material produced by the quick chilling of molten blast furnace slag through immersion in water, with or without compositional modifications, while the blast furnace slag is hot [49]. Moreover, MK is produced by burning (calcining) kaolinite clay at high temperatures between 600 and 900 ℃ [50].

The hardening of geopolymers takes place through the geopolymerization or polycondensation reaction after mixing alumina or silicate-rich materials with an alkaline activator [51]. Activators provide alkali cations that work on breaking the Si-O-Si and Al-O-Al bonds in the precursor to form the strength-giving binding phases [52,53]. Depending on the activation method, geopolymers can be divided into two-part and one-part geopolymers. A solid activator in a one-part geopolymer can be any material that elevates the pH of the reaction mixture, provides alkali cations and facilitates dissolution [52]. The most used solid activators are anhydrous sodium metasilicate and grade sodium silicate [40]. Solid activators have several benefits over liquid ones: they are easier to handle on-site,

free of hazardous highly alkaline liquids, and produced at lower cost with lower environmental impact. Incorporating a solid activator allows for easier mixing procedures similar to OPC, where the solid ingredients are dry mixed before adding the water (Fig. 1). For geopolymer 3D printing, fine aggregate with a particle size lower than 2 mm is mainly used due to the small diameter of the different nozzles used in extrusion-based 3D printing [54]. The incorporation of fine aggregate is limited, with an aggregate-to-binder ratio of 1.2–1.9 for geopolymer 3D printing [44]. The addition of additives to the mixture allows for adjusting the printed mix's rheological properties, affecting its fresh and hardened properties. The effect of different additives on the resultant mixture performance is discussed in Section 3.

3. 3D printing methods for geopolymers

During the last decade, various technological approaches have been developed for the additive manufacturing of geopolymers. There are two methods commonly used for 3D printing of geopolymer, which are (1) material extrusion and (2) powder-based technique, where the most used printing method is material extrusion [55]. The extrusion method builds the whole structure layer-by-layer by extruding materials using a hopper system with various nozzle sizes and shapes [56], as shown in Fig. 2a. The printers' mechanical parts work through a kinematic method represented by a robotic arm or a gantry. The extrusion-based gantry-type 3D printers implement a method for shifting the print head in relation to the platform along the designated coordinate axes, as shown in Fig. 3a. Multi-axis robotic arm 3D printers can enable large printing areas, which makes it possible to print accurate free-form components (Fig. 3b). However, achieving smooth movement in a robotic arm-type extrusion system is challenging compared to the gantry systems [40]. Up-to-date, the most widely used method for small to large-scale applications on- or off-site is the extrusion-based method [57].

On the other hand, the powder-based method is mainly used to produce structures with complex geometry. The 3D structure is built by introducing liquid binder into a compacted and uniformly distributed aluminosilicate precursor powder layer using a roller along a chosen path, as shown in Fig. 2b [58]. After completing designing the component, the powder residue is blown away after drying the component, as shown in Fig. 3c.

4. Fresh and hardened properties of geopolymers

Several external and internal factors can affect the fresh and hardened properties of geopolymer mixtures: the external factors include the mixing method, temperature, humidity, and curing regime, while the internal factors include the water-to-solid ratio, and the type, proportion, shape, and fineness of materials used in the precursor. Moreover, the activator's type, dosage, and molar ratio are also influential parameters. As shown in Table 1, the effect of using different mix designs on the fresh and hardened properties of printed and cast geopolymers was investigated by many researchers. Also, the effect of using different precursor types, varying precursor proportions, and incorporating retarders, superplasticizers, and other additives to obtain an optimum mixture was explored. It can be observed that the most commonly used materials in precursors were GGBS and FA. Moreover, changing the variables mentioned above influenced the fresh and hardened properties of the mixture, which are further discussed in this section.

4.1. Fresh properties

The printing requirements of a mixture are investigated by passing the mixture through the pumping, extrusion, and buildability stages. The fresh properties result and the optimal mix design of 3D printed one-part geopolymers obtained from different articles are collated in Table 2.

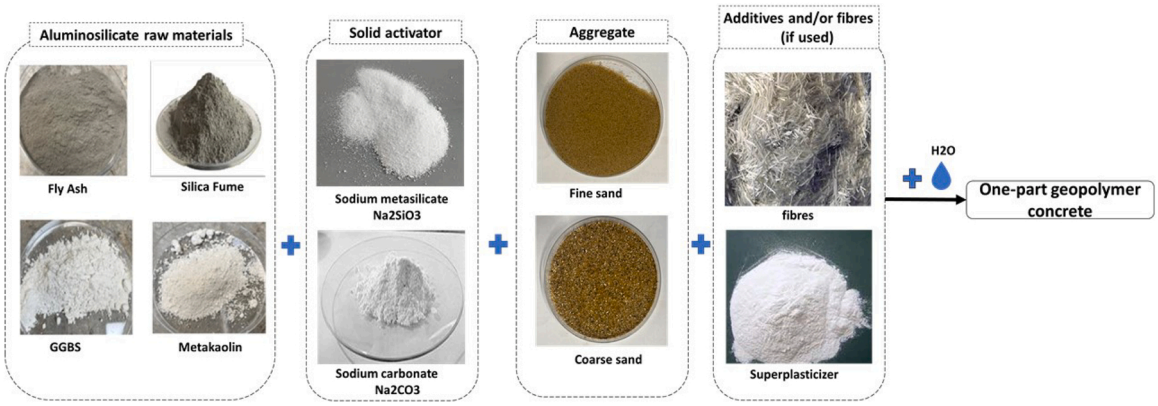

Fig. 1. One-part geopolymer preparation for 3D printing application [38].

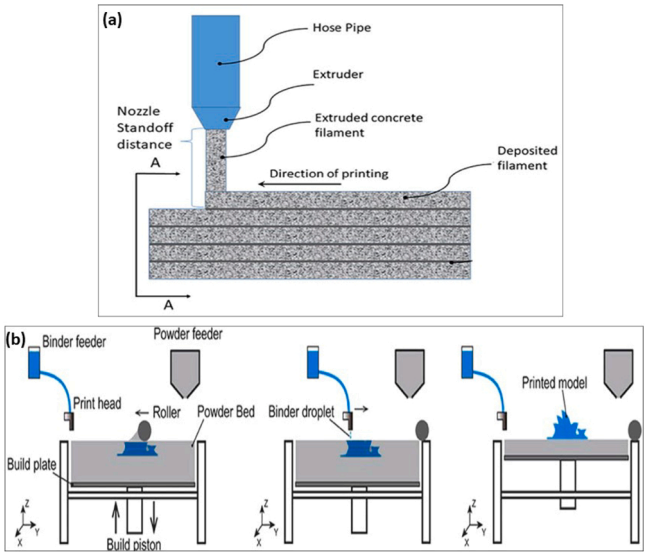

Fig. 2. Schematic illustration for (a) the extrusion-based 3D printing process [59] and (b) the powder-based printing process [58].

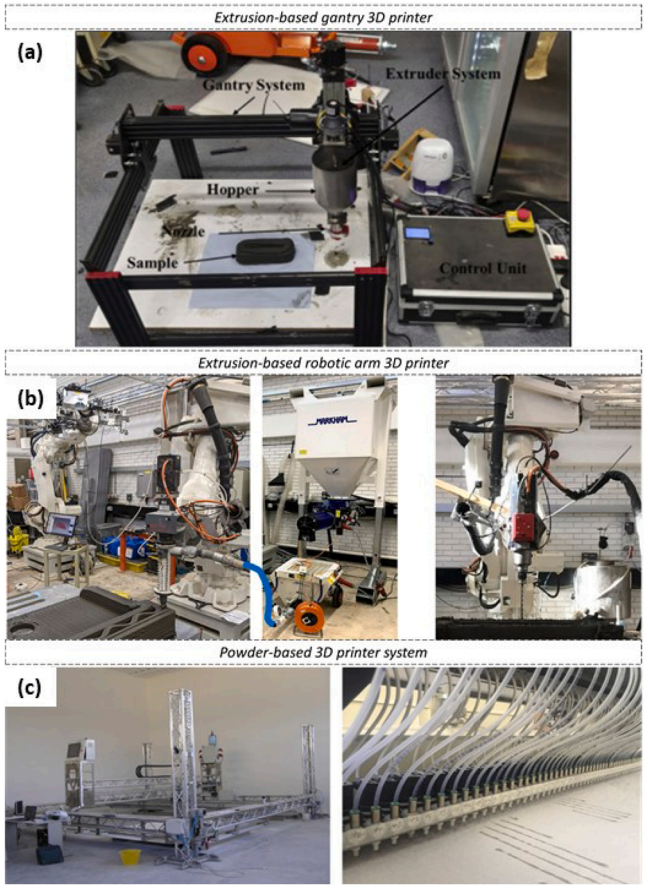

Fig. 3. 3D printing technologies: (a) extrusion-based gantry-type 3D printers [60], (b) extrusion-based robotic arm-type 3D printers [61] and (c) powder-based 3D printer [62].

Table 1
Mix formulations of one-part geopolymer.

Precursor	Activator Type	Activator percentage (%)	Aggregates size	W/b ratio	S/b ratio	Printing speed	Additives	Method	Printer type	Ref
60–85% Fly ash, 15–40% GGBS	K_2SiO_4 +KOH	10 – 20	< 2 mm	0.35	0.85	90 mm/s	-	3D printed	4 -axis gantry	[79]
50% GGBS, 50% FA 50% GGBS, 50% FA, 10% Act + 0.75% MAS + 1% sucrose	Anhydrous sodium metasilicate (Na_2SiO_3)	5 – 10	0.1–1 mm	0.36	1.5	10 mm/s	0.5 – 1.5% sucrose 0.75% thixotropic enhancer Magnesium Alumina Silicate (MAS)	3D printed	Three-axis gantry	[66]
50% fly ash, 50% GGBS	Anhydrous sodium metasilicate (Na_2SiO_3) Anhydrous sodium metasilicate + GD grade sodium silicate	8 10 0 – 7.5% + 2.5 – 10%	0.1–1 mm	0.34 0.36 0.36	1.5	35 mm/ s	- - 0.5% 1% % 0.5% Retarder	Cast and 3D printed	Gantry	[77]
80–90% GGBFS, 0 – 10% Porcelain ceramic (PC) 85% GGBFS, 5 – 10% Raw ceramic (RC)	Anhydrous sodium metasilicate Na_2SiO_3	10	0.2–1.6 mm	0.35	2	-	-	Cast	-	[80]
50 – 70% FA, 30 – 50% GGBS Cured at (20, 30, and 65 C)	Anhydrous sodium metasilicate Na_2SiO_3	8 – 10	0.1–2 mm	0.3	1	-	3 – 5% Sodium tetraborate decahydrate-Borax (retarder)	Cast	-	[67]
70 – 100% FA, 10 – 30% GGBS 60 – 80% FA, 10% GGBS, 10 – 30% SF	Anhydrous sodium metasilicate Na_2SiO_3	10	40 – 80 mesh	0.3	1.5	-	5% Commercially Attagel thixotropic thickener	3D printed	-	[19]
50% GGBS, 50% FA 50% GGBS, 50% FA	Anhydrous (AN) sodium metasilicate Na_2SiO_3 GD grade sodium silicate Na_2SiO_3	10 10	-	0.367	-	-	1% Polycarboxylate (PC1, PC2, PC3) 1% Naphthalene (N1, N2) retarders 1% Sucrose (S) 1% Borax (B) 1% Commercially (RT)	Cast	-	[76]

(*continued on next page*)

Table 1 (*continued*)

Precursor	Activator Type	Activator percentage (%)	Aggregates size	W/b ratio	S/b ratio	Printing speed	Additives	Method	Printer type	Ref
50% GGBS, 50% FA Microfibers will replace sand	Anhydrous (AN) sodium metasilicate + GD Grade sodium silicate Na_2SiO_3 (50:50)	10	0.1–1 mm	0.36 0.37 0.377 0.39 0.4 0.425	1.5	30 mm/ s	0 2.2% 4.4% 6.6% 8.8% 13.2% Wollastonite microfibers	Cast and 3D printed	Gantry	[70]
Sand replaced (S) 50% GGBS, 50% FA Precursor replaced (GP) 40 – 50% GGBS, 40 – 50% FA, 0 – 20% W	Anhydrous (AN) sodium metasilicate Na_2SiO_3	8	840 μm	0.43 0.36	1.5 1.35 1.2 1.5	-	0 10% 20% Wollastonite (W)	Cast	-	[69]
50% GGBS, 10 – 50% FA, 10 – 40% Steel slag (SS)	Na_2SiO_3 + flue gas desulfurization (FGD)	8 + 8	40 – 80 mesh	0.44	1.5	50 mm/s	-	3D printed and cast	-	[81]
100% GGBS	Sodium metasilicate	10%	-	Pastes 0.35 Mortars 0.4	0.83	60 – 100 mm/s	Nanoclay 0 – 0.6% Hydromagnesite nucleation seeds 1% and 2%	3D printed	4-axis gantry	[82]
100% GGBS	Sodium carbonate Na_2CO_3 + Calcium carbide residue (CCR)	8 + 2.5 – 10%	-	0.53	-	-	-	cast	-	[83]
100% GGBS	Na2CO3 + CCR	4 + 2.5 – 10% 8 + 2.5 – 10%	-	0.53 – 0.583	-	-	-	Cast	-	[84]
100% GGBS	Na_2CO_3 + calcined dolomite (CD)	10% + 2 – 10%	-	0.42	-	-	-	cast	-	[85]

*Alkali modulus (nSiO2/nNa2O) for anhydrous sodium metasilicate (Na2SiO3):0.9, and GD grade sodium silicate (Na2SiO3):2

Table 2
3D printed one-part geopolymers fresh properties.

Optimum mixture	Extrudability	Printability	Thixotropy	Rheological parameters	Buildability	Ref
70% FA, 30% GGBS, 10% activator	-Extruded with no breakage or discontinuity		-Increased with increasing GGBS content. -The thixotropy parameter increased with increasing activator content to 15% and decreased beyond that.	-Increased with increasing GGBS and activator level.	-	[79]
50% GGBS, 50% FA, 0.75% (MAS) thixotropic enhancer, 1.5% sucrose	-Increasing the solid activator content caused a decrement in the flowability. -The mixture with a 10% activator could not be pumped. - The addition of sucrose increased the flowability of the mix, while MAS decreased it.	-Increasing the activator dosage and incorporating MAS were found to reduce the open time of the mixture. -The addition of sucrose extended the open time.	-It was improved with increasing activator level. -The addition of sucrose was found to decrease the thixotropic parameter. -The addition of MAS was found to increase thixotropy by 200%.	-Increased with increasing activator dosage. -Yield stress was found to decrease with adding sucrose. -The incorporation of MAS increased the rheological parameters.	-It was found that using the optimum mixture can build more than 120 layers without showing any failure.	[66]
50% GGBS, 50% FA, (5 +5)% activator + 0.5% retarder	-The optimum mixture was extruded without any breakage or discontinuity.	-Retarder had prolonged the setting and open time of the mixture. -The optimum mixture open time was 65 min	-The optimum mixture had a strong thixotropy behavior. It could recover 72% of its initial apparent viscosity within 60 s	-	-94 layers were printed without observing any deformation. -More layers could be printed.	[77]
80% FA, 10% GGBS, 10% SF	-Using more than 10% SF may result in decreasing the extrudability.	-GGBS was found to decrease the initial and final setting time. Thus, limiting the open time for printing.	-Incorporating GGBS and SF was found to improve geopolymer thixotropy. - Increasing both GGBS and SF content decreased the values.	- The incorporation of GGBS and SF was found to increase both yield stress and plastic viscosity. -Increasing the replacement level of GGBS and SF decreased the results.	-	[19]
50% GGBS, 50% FA, 10% micro-fibers	-The control mix and the mixture containing micro-fibers were extruded without any blockage.	-	-The incorporation of microfibers increased the viscosity recovery, indicating the good thixotropy property of the mixture.	-Replacing sand with 10% microfibers increased static and dynamic yield strength while decreasing the plastic viscosity.	-Both the control and optimum mixture were printed successfully without deformation in the bottom layers.	[70]
-	-Increasing SS Improved extrude-ability due to the deceleration of the geopolymerization process by the presence of less reactive SS.	-The open time increased with SS content up to 20% and decreased beyond that.	-Increasing SS content improved the thixotropy property.	-Plastic viscosity and static and dynamic yield stresses decreased with SS content.	-The buildable height increased with SS content up to 10% and then decreased when printing free wall. -When printing square walls, the buildable height decreased with SS content.	[81]
100% GGBS, 0.4% NC, 2% seeds	-Increasing the NC content to 0.6% led to the extrusion of discontinuous filaments. -	-The optimum printing speed was set to 90 mm/s to print layers with the same width as the nozzle inlet.	-NC improved the viscosity recovery behavior of the mix by 25% due to its thixotropy property.	-Although 0.6 resulted in the maximum yield stress, 0.4% was selected as the optimum. -NC inclusion resulted in three times higher yield stress without affecting the apparent viscosity. -The incorporation of the accelerator slightly affected the yield stress.	-A 15 layers cylinder was printed using the mix with NC to investigate the efficiency of printing speed, and no deformation was observed. -Twisted column was printed without having any deformation in the bottom layer.	[82]

4.1.1. Pumpability and extrudability

Pumpability is the process that transports the workable mix through a pipe from the reservoir to the nozzle under pressure without affecting the materials` properties (workability and yield stress) for the entire transporting time [63]. At the same time, extrudability is defined as the ability of the mixture to be extruded from the nozzle smoothly under pressure in good quality without altering the mixture's physical properties [64], where a good quality extrusion refers to filaments that have been extruded without any breakage or discontinuity [45]. The requirements of printable material are somewhat contradictory; the mixture must be workable enough to ensure ease of transportation prior to extrusion, and the extruded mixtures must retain their shape by being relatively stiff [65]. The rheological performance of materials and the mix design affect pumpability and extrudability, where the desired mixtures should have low viscosity and optimum yield stress for easy pumping and extrusion, as shown in Fig. 4 [6]. Muthukrishnan et al. [66] investigated the effect of increasing the activator content on the pumpability of GGBS and FA one-part geopolymer by measuring the static yield strength with time. It was found that increasing the activator content resulted in a faster evolution of yield stress, thus, increasing the pumping energy required. Different articles aimed to determine the effect of several precursor materials and found that enriching the mix with materials containing calcium, like GGBS, decreases the extrudability. Guo et al. [19] found that the incorporation of up to 10% SF in FA-based one-part geopolymer improves the particle packing and enhances the viscosity, but due to its fine particle size, increasing the SF ratio results in decreasing the viscosity. Accordingly, using more than 10% of SF in the mixture may result in the decline of extrudability due to excessive viscosity loss. Shah et al. [67] found that increasing GGBS percentage in the mixture resulted in a decrease in flowability, which could be due to the presence of more nucleation sites at the early stage that additional calcium in GGBS provides, thus, resulting in the rapid hardening of the mixtures [67]. Additionally, the workability tends to decrease due to the GGBS's angular shape [68].

Bong et al. [69] studied the effect of replacing precursor and aggregate separately with wollastonite powder on the workability of FA- and GGBS-based one-part geopolymers. The results showed that increasing the replacement level decreases the spread diameter by forming network structures that can resist the flow due to the needle-like shape of wollastonite. In another study, Bong et al. [70] investigated the effect of replacing fine natural sand with wollastonite microfiber on the extrudability of FA- and GGBS-based one-part geopolymers by printing five layers of square slabs with a total length of 4810 mm for each layer. The mixture with a 10% replacement level was found to have comparable workability with the reference mix, and the researcher successfully extruded the reference mix and the mixture with a 10% replacement level. On the other hand, the pumpability can be improved by increasing the water/binder ratio. However, increasing water content beyond a certain level may result in segregation and pipe blockage [71,72]. On a positive note, incorporating retarders can enhance extrudability by slowing the reactions [67]. In a recent study, Cheng et al. [73] investigated the effect of adding different types of superplasticizers (namely, polycarboxylate (PC), melamine (M), and naphthalene (N)) with different dosages on the flowability of calcium carbide residue–waste red brick powder-based one-part alkali-activated materials. The authors found that adding 1.5% PC among the different types significantly increased the flowability of the mixtures to a comparable level to the OPC mixture. Similarly, Alrefaei et al. [74] studied the effect of incorporating PC, M and N superplasticizers on the mini-slump performance of FA-GGBS-based one-part geopolymer and found that the flowability of the mixtures improved, where poly-carboxylate showed the most significant improvement.

4.1.2. Shape retention

Shape retention is known as the ability of the extruded layer to resist deformation and maintain its cross-section compatible with the nozzle cross-section. The deformation of the deposited layer can result from three main factors: the weight of the layer itself, the weight of the succeeding layers, and the pressure applied during the extrusion process [75]. The shape retention of a mix can be improved by using materials that can enhance the thixotropy property of the mixture. For instance, Bong et al. [76] found that replacing sand with 10% wollastonite enhanced the shape retention ability of the mixture due to the enhancement in thixotropic behavior and yield stress. While Guo et al. [19] stated that incorporating GGBS in an FA-based one-part geopolymer can enhance the thixotropic behavior of the mix, thus, enabling the mix to maintain its shape. Additionally, the presence of fine SF particles improves the mixtures' packing density, which results in better yield stress, where the higher yield stress helps maintain the shape of the printed layers. Muthukrishnan et al. [66] found that increasing the activator content enhances shape retention after extrusion by the rapid re-flocculation of the mix. Bong et al. [77] evaluated the shape retention ability of FA- and GGBS-based one-part geopolymer by adding

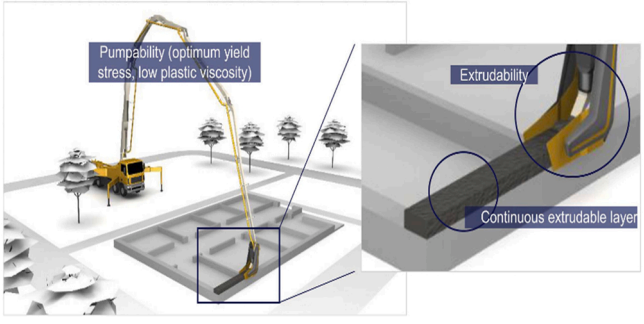

Fig. 4. Materials properties required for the pumping and extrusion process [6].

a steel plate on top of a cylinder-shaped mixture and recording the deformation every 30 s before adding another steel plate. The mixture had a deformation of 3.9% in width and 10.4% in height immediately before collapse. Moreover, the results showed that the mixture had a good shape retention ability which collapsed after applying a load that equals around nine times its self-weight. The shape stability of the mixture can be enhanced by incorporating additives, such as MAS, Poly-vinyl Alcohol (PVA) fibers, attapulgite nano clay, and nano graphite platelets [60,66,78]. Further study is necessary to investigate the impact of different mixing times and speeds on the 3D-printed layers' shape retention.

4.1.3. Open time and setting time

Open time is when the material is extrudable after adding water to the mixture; beyond that time, the material loses its extrudability. The suitable open time of the material has to be sufficient to contain the period for which the material is to be deposited. Otherwise, the material will harden in the nozzle or container [60]. Open time and setting time depend mainly on the mix design. Depending on the type of precursors used, the open time and setting time of one-part geopolymers changes according to the rate of the mixture reaction mechanisms. One of the main differences between precursors rich in GGBS and other precursors is their setting time, where the presence of rich-calcium material results in the faster setting of the mix [68,86,87]. Shah et al. [67] reported that increasing GGBS shortens the setting time of the mix because of the rapid hardening due to the additional reactions that GGBS imposes at the early stage. In addition, Panda et al. [79] stated that the amount of GGBS in the precursor should be controlled because it can change the flow properties, thus, significantly affecting the open time of the mix.

Similarly, the activator content has an inverse relationship with open time. Muthukrishnan et al. [66] reported that the increment in activator percentage limits the open time of the mix due to the rapid evolution of yield strength. To extend the open time, they investigated the effect of incorporating a retarder and found it to slow the yield strength development, which increases the open time. Ma et al. [81] studied the effect of replacing up to 40% of FA with steel slag and found an increment in open time, which could be due to the deceleration of the geopolymerization process caused by the presence of steel slag. However, it was found that using more than 20% replacement level decreased the flowability of the mixture, consequently decreasing the open time, as shown in Fig. 5.

The studies on the open time of one-part geopolymers are limited. Further research is required to understand the effect of different precursor types, mix designs, additives and retarders on the open time of one-part geopolymers.

4.1.4. Rheological properties

The main rheological properties are plastic viscosity, yield stress, and thixotropy. Yield stress is divided into static and dynamic yield stress. Static yield stress is the shear stress needed to start the mixture's flow. After the flow starts, the needed shear stress for maintaining that flow is called dynamic yield stress. 3D printable concrete flows when applying external shear stress [88,89], where the mix stop flowing after removing the external force, and thixotropy occurs. Thixotropy is a phenomenon where the mix restores static yield stress by initiating flocculation of the particles due to inter-particle interaction [90]. Rheological properties mainly depend

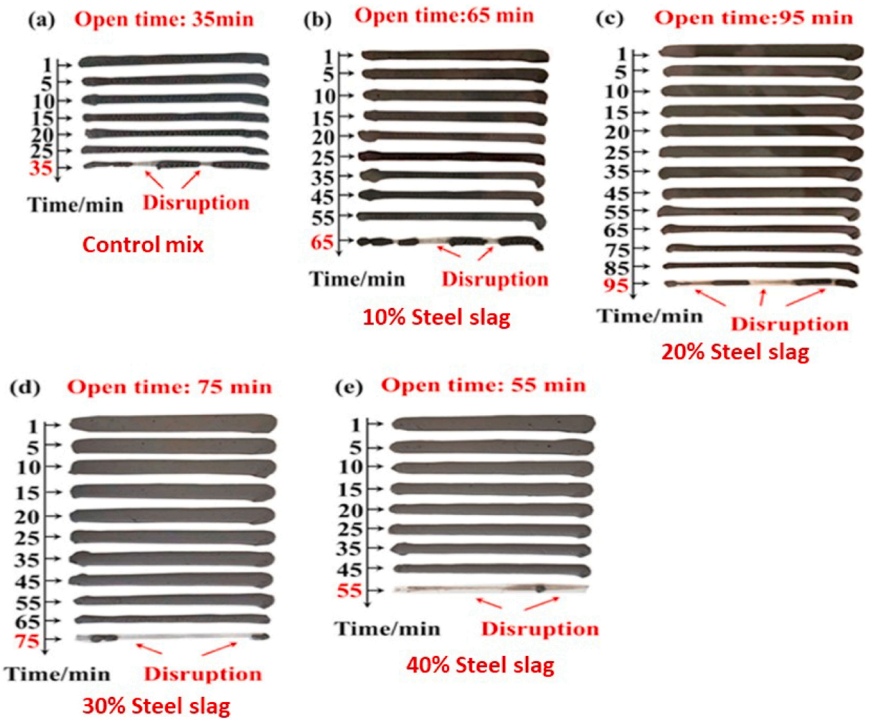

Fig. 5. Effect of replacing FA with different steel slag content on open time of one-part [81].

on the mix design of the fresh geopolymer and the shape of the solid ingredients of the mixture. Panda et al. [79] observed that increasing GGBS content in FA-based one-part geopolymer increased yield stress, plastic viscosity, and viscosity recovery, which is due to the chemical composition of GGBS that is rich with calcium. Due to the angular morphology of GGBS particles, the packing density increases, enhancing the mix's thixotropic property.

Kaze et al. [91] compared the rheological behavior of lateritic clay (LAC)- and iron-rich laterite clay (LAI)-based geopolymers. The results revealed that LAI possesses significantly higher yield stress than LAC, which is justified by the higher deformation that LAI exhibited due to the higher interaction rate between its different constituents since iron (Fe) possesses a higher reaction rate than Si and Al. Thus, iron species quickly precipitate in an alkaline medium to form iron hydroxide gel, accelerating the polycondensation process and producing a more rigid structure. In another study, Kaze et al. [92] studied the effect of different calcination temperatures on the rheology of meta-halloysite-based geopolymer and found that increasing the calcination temperature improved the rheological behavior of the geopolymer due to the increase of the reactive phases. Ma et al. [81] found that replacing FA up to 100% with steel slag in FA- and GGBS-based one-part geopolymer decreased the rheological properties of the mix. The decrement could be due to the steel slag's low reactivity, which prevented FA and GGBS from reacting with the activator and producing the hydration gels. Moreover, Bong et al. [70] found that replacing 10% of fine sand with wollastonite microfiber in FA and GGBS-based one-part geopolymer increased yield stress and decreased the plastic viscosity of the mix. The increased yield stress could be due to physical interlock and overlap between wollastonite acicular particles. At the same time, the plastic viscosity decrement could be due to the more elongated particle shape of wollastonite compared to the mixture's other solid particles. Moreover, it was found that substituting sand with 10% fibers had slightly enhanced the thixotropic property and resulted in recovering 80% of the viscosity. Besides the effect of different precursor materials, activator content has an evident effect on the rheological behavior of the mix. Muthukrishnan et al. [66] found that increasing the activator content significantly increased yield stress and viscosity and improved the thixotropy of the mixture [66]. However, using higher activator percentages may decrease the plastic viscosity of the mix [79]. The activator composition (i.e., alkali modulus) also plays a crucial role in influencing the rheological properties of the geopolymer. According to [93,94], increasing the SiO_2/Na_2O ratio increased the viscosity and yield stress of the geopolymer mixture.

4.1.5. Buildability

Buildability is the ability of 3D-printed filaments to retain their shape and resist distortion induced by both their weight and the weight of the succeeding layers after it has been extracted from the nozzle [88]. As stated in section 3.1, the mixture must possess high-yield stress after extrusion to retain its shape. In order for the first layer to withstand the weight of the subsequent layers, the mixture should have enough early strength. The buildability mainly depends on the mixture's rheological properties and object design, including geometry, size, and process parameters [95]. Muthukrishnan et al. [66] investigated the effect of different activator percentages on the buildability of FA- and GGBS-based one-part geopolymer by evaluating the static yield stress development over time when changing activator content. They validated the results by conducting a 3D printing test to determine the maximum number of layers that can be printed before the collapse of the structure or the deformation of bottom layers to 0.5 of the layer's initial width. It was found that increasing the activator content resulted in a faster yield stress growth over time, which improved the retention of the mix and allowed for more layers to be printed. They also investigated the effect of incorporating nano-clay and sucrose and found that adjusting and balancing these additives can allow printing more layers (as shown in Fig. 6). Although adding 1% sucrose increased the open time, the yield stress development rate and thixotropy were decreased and resulted in limiting the number of layers that could be printed (Fig. 6c). Furthermore, incorporating 0.75% nano-clay resulted in a better yield strength development and thixotropic behavior for the mix with sucrose. At the same time, it limited the open time of the mix. Adjusting sucrose to 1.5% resulted in producing a mix with comparable properties to the control mix with adequate open time, which allowed the printing of 120 layers for one patch without failing (Fig. 6d). Chougan et al. [60] proposed incorporating nano-graphite to enhance the buildability of 3D printed geopolymer.

Bong et al. [77] studied the buildability of FA- and GGBS-based one-part geopolymer when combining 5% anhydrous sodium metasilicate and 5% GD grade sodium silicate activator by printing a rectangular column and found that the mixture had excellent

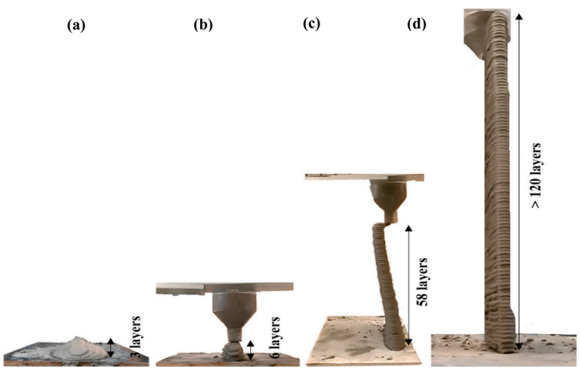

Fig. 6. Buildability test of a) 5%ACT (activator), b) 7.5%ACT, c) 10%ACT-1%S (sucrose), and d) 10%activator-1.5%S-0.75% thixotropic enhancer one-part geopolymer mixes [66].

Table 3
One-part geopolymer hardened properties.

Optimum mixture	Compressive strength	Flexural strength	Ref
70% FA, 30% GGBS, 10% activator	-Increased with increasing GGBS and activator. -Strength at the printing direction was the highest.	-	[79]
50% GGBS, 50% FA, 0.75% (MAS) thixotropic enhancer, 1.5% sucrose	- The compressive strength results in all directions were higher than printed geopolymer in other studies at 7 and 28 days.	-A higher strength was obtained at 7 and 28 days compared with similar geopolymers from other studies.	[66]
50% GGBS, 50% FA, (5 +5)% activator, 0.5% retarder	-Cast specimens had higher strength values compared with the printed one. -The X-direction had the highest value among the other directions. (X-direction load was in the plane of the interfaces between layers). Y-direction was the printing direction, and Z was perpendicular to it.	-Y and Z-direction had higher strength values compared with x-direction and the cast specimen. -Y-direction had the highest value, followed by Z, cast specimen, and x-direction, respectively.	[77]
85% GGBFS, 10% PC	-Sealing specimens in plastic bags were found to have the highest strength values compared with submerging and ambient curing methods. -The highest compressive strength was obtained when replacing slag with fired ceramics by 10%. -All the values were lower than the control specimen.	-Specimens sealed in plastic bags had the highest strength. -All values of specimens sealed in plastic bags were slightly lower than the reference mix.	[80]
60% FA, 40% GGBS, 10% activator, 4% retarder	-The strength values increased with increasing slag and activator content. -Using more or less retarder content than 4% decreases the strength values. -Compressive values increased with increasing curing temperature at early ages. -At 28 days, the curing temperature did not affect strength values.	-Increasing slag and activator content resulted in a drop in the flexural values. - Flexural results were found to be decreased when using retarder content other than 4%. -At an early age, flexural strength increased with increasing curing temperature. -At 28 days, flexural strength was not affected by curing temperature.	[67]
50% GGBS, 50% FA, PC1 50% GGBS, 50% FA, S	-GD Grade sodium silicate was found to have higher strength values than the anhydrous activator. -The incorporation of superplasticizer (SP) did not affect the mixtures activated with AN, while it reduced the strength values of mixes activated with GD-grade sodium silicate -The incorporation of (R) retarders did not affect the mixes activated with anhydrous sodium silicate (AN), while decreased strength of mixes activated with GD. -The combination of SP and R decreased the compressive strength values compared to using them separately.	-	[76]
50% GGBS, 50% FA, 10% microfibers	-Comparable strength values were obtained with increasing sand replacement levels with microfibers for cast specimens. -For printed specimens, adding wollastonite did not affect the compression performance, where both mixtures exhibited similar strength values. -The highest strength values were obtained in the X-direction (Printing direction)	-For cast samples, flexural strength values increased in the presence of microfibers compared with the control specimen, where the highest value was obtained when replacing 10% sand. -The strength results were comparable to the control specimen for printed specimens. The strength values of the mixture containing wollastonite in the Y and Z directions were slightly higher than the control specimen. -The highest strength values were obtained in Z-direction.	[70]
GP + 10% wollastonite (W)	-Higher compressive values were achieved in mixtures that replaced precursor (GP) with wollastonite (W) than mixtures that replaced sand (S) due to the lower water content in GP. -The highest values for S and GP mixtures were obtained using 10% wollastonite.	-GP had higher flexural strength than S due to the lower water content. -The incorporation of W increased strength in S mixtures while not affecting GP mixtures. -For S mixtures, the highest flexural value was obtained when replacing 20% of sand. While for GP, all the results were comparable.	[69]
-	-At 7 days, the compressive strength increased with increasing SS to 30%. While the 28-day compressive strength decreased with SS content, the highest value was obtained when adding 10% SS. - The results of all directions were higher than the casted specimen, where Y-direction had the highest results among all directions.	-The flexural results for 3D printed specimens in all directions were lower than the casted sample.	[81]
-	-Increasing the CCR ratio (i.e., 7.5% and 10%) decreased the compressive strength of the samples in the different curing methods when immersed in water and aggressive ambient (i.e., Na_2SO_4 and $MgSO_4$). -Compressive strength values significantly decreased when immersing samples in $MgSO_4$ -Compressive strength loss at 84 days increased with increasing CCR ratio when exposing mixtures to Na_2SO_4.	-	[83]

(*continued on next page*)

Table 3 (*continued*)

Optimum mixture	Compressive strength	Flexural strength	Ref
100% GGBS, 8% Na_2CO3, 2.5% CCR	-The compressive strength significantly increased with increasing the activator ratio from 4% to 8%. -For the 4% activator ratio, the incorporation of 5% CCR had the highest development in compressive strength at early ages. However, 2.5% possessed the highest compressive strength at later ages. -For the 8% activator ratio, 2.5% and 5% exhibited the highest compressive strength, while 2.5% had the highest results at 28 days.	-	[84]
100% GGBS, 10% CD	-Increasing CD content increased the compressive strength performance of the mixtures, where 10% achieved the highest values. -All mixtures with the different CD ratios exhibited noticeably higher strength values than NaOH solution-activated slag and less compressive strength than Na_2SiO_3 solution-activated slag.	-	[85]

buildability. Moreover, Panda et al. [79] estimated the buildability of a one-part geopolymer by determining its load-carrying capacity in the dormant period. The dormant period before the mix setting was found to be less than 30 min, referring to the fast development of early strength, which could be due to the initial stage reaction that produced aluminosilicate gel.

4.2. Hardened properties of one-part geopolymers

Mechanical strength tests on 3D printed specimens were assessed by applying load in three directions; longitudinal, lateral, and perpendicular to the printing direction, which are called X, Y, and Z, respectively. Specimens have been extracted with different dimensions from printed blocks depending on the type of test to be conducted. The effect of using different mix designs on the hardened properties of printed and cast geopolymers was investigated by different researchers, as shown in Table 1. The effect of using different precursor types, varying precursor proportions, and incorporating retarders, superplasticizers, and other additives to obtain an optimum mixture was explored. The mechanical performance along with the optimal mix design obtained from different articles for 3D printed and cast one-part geopolymers are shown in Table 3.

4.2.1. Compressive strength

Several studies have shown that comparable strength values can still be obtained by controlling the printing parameters and mix design [3,60]. Depending on the mix design, the strength of a one-part geopolymer is often higher when using a calcium-rich precursor. That is in good agreement with the results obtained from different articles shown in Table 3. The more incorporation of GGBS, the higher the compressive strength [60,96]. However, increasing GGBS beyond a certain limit causes a decrement in the compressive strength, which could be due to the loss of workability, as illustrated in Fig. 7(a). Panda et al. [79] found that increasing GGBS content from 15% to 40% significantly increased the compressive strength values of FA-based one-part geopolymer due to the early formation of C-S-H. They also found that strength values tend to increase when rising activator dosage from 10% to 20% due to the more Si ions available for geopolyermization. Determining the optimum precursor proportion for a specific activator percentage and water amount may lead to optimized compressive strength [97]. Dong et al. [97] found that the fineness of the materials plays a significant role in improving the mechanical strength of the geopolymer, where using a finer activator significantly increases the compressive values of

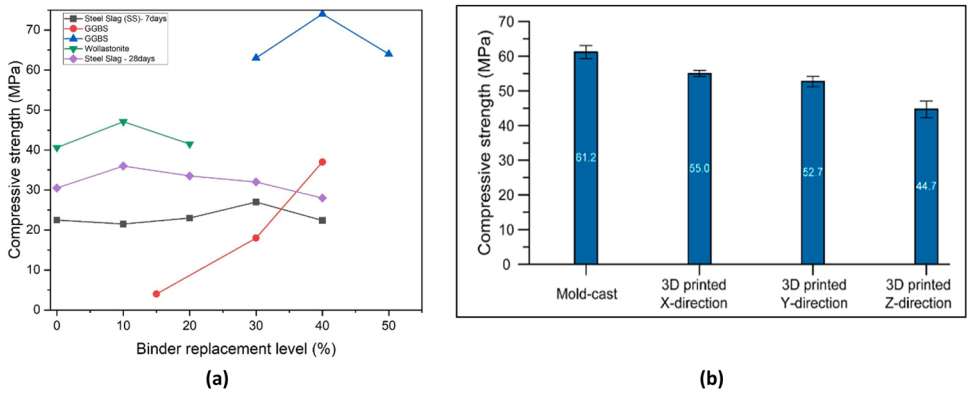

Fig. 7. Compressive strength of one-part geopolymers with (a) cast specimens when precursor partially replaced with different materials [67,69,79,81] and (b) different directions on 3D printed optimum mixtures [77].

one-part geopolymer. Moreover, the compressive strength is affected by the used activator type, where the most effective and used solid activator is sodium silicate. Ma et al. [98] found that partially replacing Na_2SiO_3 with Na_2CO_3 decreased the compressive strength of one-part geopolymers due to the decrease in the geopolymerization degree in the presence of Na_2CO_3. The incorporation of retarders and rheology-modifying admixtures can result in decreasing the compressive strength value. Sun et al. [99] studied the influence of using up to 8% viscosity modifying admixture on the mechanical properties of one-part geopolymer and found that the compressive strength decreases with increasing the additive dosage. The decline in the strength values in the presence of a modifier was attributed to the aeration effect and the creation of a dense polymer film that hinders the contact of silicate powder with the activator [99].

On the other hand, various researchers studied the effect of using waste material to replace aggregates or part of a precursor. Abdollahnejad et al. [100] found that replacing up to 30% of GGBS with fired and unfired ceramic reduced strength values in GGBS-based one-part geopolymer. While replacing natural aggregate may increase or decrease the strength depending on the type of aggregate used [101].

Fig. 7b shows the anisotropic compressive strength behavior in different testing directions. Some studies found that printed specimens exhibit higher compressive strength values when tested longitudinally (X-direction) to the print direction compared to cast specimens and the other directions. This can be due to the movement patterns, as the materials move in the direction of printing, allowing for more compaction after placing the particles compared to the other direction [79]. The characteristics of the printing process result in an anisotropy behavior dependent on the direction of testing [102,103]. This anisotropic nature of printed structures may be explained by the heterogeneity created by the interaction between layers. Due to the intense pressure during the extrusion, the 3D-printed object has a denser microstructure than cast concrete. Nevertheless, the printed object has higher porosity with weaker connections at the layer interface [104]. Other studies [70,77] reported higher compressive strength values for cast specimens than that of 3D-printed one-part geopolymers, which could be due to the higher porosity of printed samples compared to the cast ones.

4.2.2. *Flexural strength*

Like compressive strength, flexural strength was found to increase with increasing the activator content and Ca-rich materials [105]. While Shah et al. [67] observed a decrement in the flexural strength when increasing GGBS content, as shown in Fig. 8a, due to the low water content used in the mix. Moreover, Fig. 8a presents the effect of replacing precursors with different materials on the flexural strength of cast specimens. Flexural strength was also found to follow an anisotropic behavior dependent on the testing direction, as shown in Fig. 8b. Most studies revealed that 3D printed specimens had a slightly higher flexural strength when the load was applied lateral (Y) and perpendicular (Z) to the printing direction. The lowest flexural values are observed when the load is applied in the X-direction, which can be due to the weak interface between layers [57,106,107]. In 3D printed elements, two different interfaces are produced: a horizontal interface is produced by extruding the subsequent layer on top of the previous layer, and a vertical interface is formed between two layers when the subsequent layer is placed next to the previous layer at the same level. The strength at the center of the extruded concrete is greater than that at the layer interfaces [57,104]. Different researchers investigated the effect of using fibers to enhance the flexural strength of 3D-printed concrete. They found that incorporating fiber enhanced the printed filaments in perpendicular and lateral directions while not changing the observed anisotropy trend [108,109]. Bong et al. [70] studied the effect of replacing the finest sand with up to 30% wollastonite microfibers on the flexural strength of 3D-printed one-part geopolymer and found that replacing 10% of sand resulted in the highest flexural strength values. The strength was around 4 MPa higher than the reference mix for cast specimens and 1.5 MPa, and 0.5 MPa higher for 3D printed specimens in Z- and Y-directions, respectively. The enhancement can be due to the connection of wollastonite particles to the geopolymer matrix after being partially dissolved in the mixture. The presence of these particles in the mixture is supposed to be helpful in crack bridging and crack blocking through the fraction deflection and fiber rupture, which increases the load needed to rupture [75]. Ma et al. [81] found that the lower flexural strength values of 3D printed one-part geopolymers in all directions than the cast specimens are due to the presence of extra air voids during the printing process and the generation of weak interlayers in the bottom.

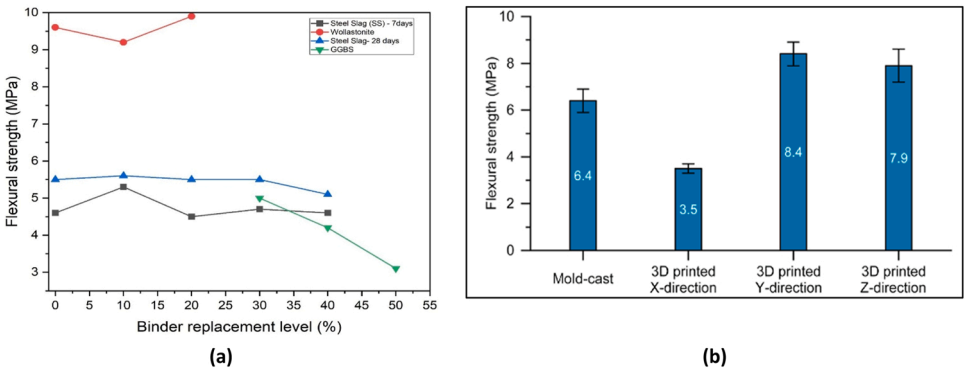

Fig. 8. Flexural strength of one-part geopolymers with (a) cast specimens when precursor partially replaced with different materials [67,69,81] and (b) different directions on 3D printed optimum mixtures.

5. Economic assessment of one-part geopolymers

One of the main benefits of using 3D printing technology could be the reduction in the overall cost. The involvement of 3D printing provides more economical solutions in terms of material saving, required effort, and energy. Concrete 3D printing (3DCP) does not require formwork, which accounts for 10% of the overall cost. Due to the elimination of formwork, the formwork labor will be no longer needed, reducing the overall cost by 50% or more, as highlighted in [21]. Batikha et al. [110] compared different building techniques and showed that 3DCP is more economical than other construction techniques. According to the study, construction cost is responsible for 55% of the total cost and the material cost for 45% (see Fig. 9). Other researchers found that the construction cost consumes 70% of the total cost when using a robotic arm for 3DCP [13,111].

The total cost of construction when using 3DPC can also be decreased by employing different approaches, including printing hollow structures and using AAMs to reduce the cost of printing materials [44,112]. Using recycled aggregate, coarse aggregate, and industrial by-product materials can also reduce the total cost [113]. However, Abbas et al. [114] found that producing 1 m^3 concrete with metakaolin geopolymer is three times higher than the total cost of producing it with OPC. This is due to the high cost of geopolymer materials, where sodium hydroxide contributed to 41% of the total cost, metakaolin by about 31%, and sodium silicate by about 19%. Yang et al. [115] showed that the type and content of alkali activators affect the production cost of alkali-activated GGBS. They found that the cost of one-part alkali-activated blast furnace slag foamed concrete was slightly higher than that of OPC concrete. Ma et al. [116] compared the cost of producing 1 m^3 one-part geopolymers prepared with different sodium metasilicate types and 1 m^3 OPC concrete and found that one-part geopolymers had higher costs than OPC concrete. In contrast, Habert and Ouellet-Plamondon [117] compared the economic allocation of one-part geopolymers with OPC and found the possibility of reducing costs by 80% compared with OPC. Vinai et al. [32] compared the costs of production and raw materials of one-part alkali-activated concrete (AAC), Portland cement concrete (PCC), and two-part alkali-activated concrete. The results showed that two-part had the highest cost, while one-part AAC had a slightly lower cost than PCC at all concrete strengths. The low overall cost of one-part AAC is due to the low price of sodium silicate powder, which is four times lower than sodium silicate solution. Based on the above-presented articles, the implementation of solid activators can reduce the overall cost of the one-part geopolymers to a comparable level and even lower than OPC, depending on the used precursor.

* 3DPC: 3D concrete printing, PMC: prefabricated modular construction, CFS: cold-formed steel, and HRS: hot-rolled steel.

6. Environmental impact of one-part geopolymers

3D concrete printing is the most sustainable construction method, which produces a lower amount of CO_2 compared with other types of construction [110]. Mohammad et al. [118] compared reinforced concrete (conventional method) with 3D concrete printing and found that 3D printing concrete produced around 22% less carbon dioxide emissions. Due to the higher amount of cementitious binder in 3D concrete printing technology than in conventional concrete [119], the researchers have focused on finding more environmentally friendly materials instead of cement due to the consumption of around 4% of greenhouse gas (GHG) and to the release of around 8% of the total global CO_2 emissions associated with cement production [120].

Yoa et al. [121] found that using geopolymer in 3D printing decreases the overall CO_2 footprint of concrete production. However, an increase in the use of abiotic resources and depletion of stratospheric ozone was observed. Moreover, Liu et al. [122] found that cast geopolymers had lower environmental impacts than the cast OPC sample, while it did not outperform OPC when printed due to the higher activator content in the mixture. However, when constructing a wall, the environmental impact of the casting technique varied depending on the shape complexity while remaining constant for the 3D printing method [122].

According to the literature, most of the articles used the combination of sodium hydroxide (NaOH) with sodium silicate (Na_2SiO_3) to produce the liquid activator used in two-part geopolymers because the use of NaOH only cannot enhance the strength significantly

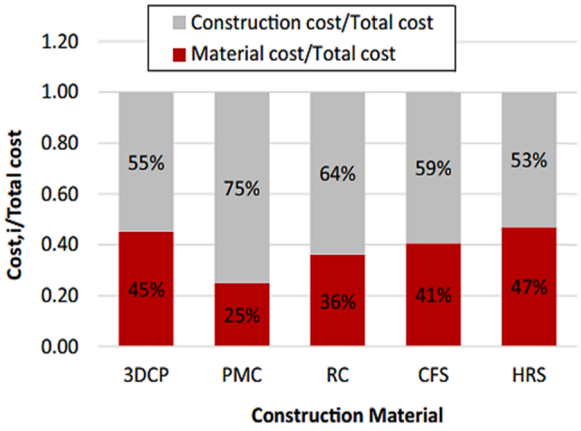

Fig. 9. The relative percentage of the material cost (USD) and construction activity of total cost (USD/m^2)* [110].

[123]. Using one-part geopolymers eliminated the need for combining them, resulting in a more environmentally friendly mix than two-part geopolymers. The environmental impact key contributor to geopolymers is the production of alkali activators, as reported in [124] and [125]. The CO_2 emissions produced by activators vary depending on the type of activator, where the CO_2 inventory of Na_2SiO_3 was found to be higher than that of $Ca(OH)_2$ [115]. Furthermore, one-part alkali-activated slag foamed concrete had 85 – 93% lower CO_2 emissions, depending on the type of activator used, compared to that of OPC [115]. The production of 3D printable one-part geopolymer mixes prepared with a solid activator can reduce up to 70% of the carbon emissions and 15% of embodied energy compared with 3D printable OPC having a similar compressive strength value [126]. Panda et al. [79] found that a one-part geopolymer sample had lower CO_2 emissions of around 78%, and the embodied energy accounted for about 15% of that for the OPC-based specimen. Moreover, they revealed that the activator had around 81% of the total energy of the overall mix [79]. Ma et al. [116] calculated the embodied CO_2 index of one-part geopolymers prepared with various types of sodium metasilicate with and without water in their chemical compositions. It was found that one-part geopolymer mixes prepared with different types of sodium metasilicate had lower CO_2 emissions per MPa for 1 m^3 compared to OPC. Although sodium metasilicate with water had the highest CO_2 emission among the other types, it was found to have the lowest embodied CO_2 index when used in the mix [116]. Luukkonen et al. [38] calculated the average environmental impact obtained from different studies and showed that the environmental impact of one-part geopolymers was 24% less than that of OPC, which is lower than the environmental impact of two-part geopolymers, which was 60% of the environmental impact of OPC. It is evident from the different results that using a solid activator to produce a one-part geopolymer is assumed to be an excellent solution to decrease the environmental impacts due to the benefits it presents compared with OPC and two-part geopolymers.

Incorporating a one-part geopolymer in construction applications can be a potential and feasible solution to meet the goals, of the European Cement Association, of decreasing the carbon footprint of cement to more than half by 2030 [127] due to the use of low-carbon materials in the mix. In addition, using one-part geopolymers is comparable and even more economical than OPC in industrial applications.

7. Conclusions and future directions

Implementing a one-part geopolymer in 3D printing technology offers several advantages over conventional geopolymer and concrete. The focus of this paper was mainly on the fresh and hardened properties of different mix designs of 3D printed one-part geopolymers, their environmental impact, and their cost assessment. From this review, the following conclusions can be drawn:

1. Utilizing GGBS in one-part geopolymers can enhance the mix's properties. However, it decreases the open time and extrudability.
2. Increasing activator content can improve the rheological properties and mechanical strength of one-part geopolymers while decreasing the open time and flowability, thus, limiting the printability of the mix.
3. Retarders and superplasticizers can be used to extend the open time and increase the flowability of a mix, but they will decrease yield stress, thixotropy, and mechanical strength of the mix.
4. One-part geopolymers have slightly lower mechanical strength than two-part geopolymers but are still stronger than OPC.
5. Depending on the type of materials used in the precursor, one-part geopolymer can result in reduced costs compared to OPC-based concrete samples. The most expensive material in OPC is cement, while for the geopolymers, it is the activator.
6. Incorporating a solid activator leads to around half of the environmental impact produced by a liquid activator, making one-part geopolymers a more environmentally friendly mix. It also allows for practical use on a large scale due to eliminating the liquid activator risk.

Based on the presented review, besides the successfully developed one-part geopolymer mixtures for 3D printing, some challenges need further consideration in future research. Despite the good mechanical behavior of one-part geopolymers, further research is needed to eliminate the mechanical anisotropic behavior of 3D printed filaments by conducting more studies on the effect of different printing parameters and the incorporation of fiber reinforcement. Moreover, the durability of 3D-printed one-part geopolymers needs to be investigated since most studies focus on evaluating the mechanical properties, mainly compressive strength. The effect of incorporating different nano-particles on the fresh and hardened properties can also be investigated. Most researchers focused on investigating the effect of different mix designs on the mechanical and rheological properties of 3D printed one-part geopolymer. Its good performance and similar preparation procedures to OPC make it a suitable alternative in 3D printing for different industrial applications, including prefabrication and onsite construction. While open time had rarely been investigated and mostly had a narrow window when a solid activator is presented due to the rapid yield stress development, which restricts the use of one-part geopolymers in the 3D printing application. Therefore, the effect of different parameters on the open time is to be investigated to develop a one-part geopolymer mixture with an adequate printing window to address this problem and to be used in building applications. Furthermore, the problem of limited open time for printing needs to be solved by investigating the effect of different types and dosages of retarders and superplasticizers, incorporating various materials in precursors, and changing the preparation parameters.

CRediT authorship contribution statement

Yazeed A. Al-Noaimat: Data curation, Methodology; Validation, Investigation, Writing – original draft, Visualization. **Seyed Hamidreza Ghaffar:** Conceptualization, Methodology, Supervision, Writing – review & editing, Resources, Writing – original draft, Visualization, Supervision, Funding acquisition. **Mehdi Chougan:** Writing – review & editing, Data curation. **Mazen J Al-Kheetan:**

Writing – review & editing, Validation.

Declaration of Competing Interest

The authors declare that they have no known competing financial interests or personal relationships that could have appeared to influence the work reported in this paper.

Data Availability

Data will be made available on request.

Acknowledgements

This work was funded as part of the DigiMat project, which has received funding from the European Union's Horizon 2020 research and innovation program under the Marie Skłodowska-Curie grant agreement ID: 101029471.

References

[1] L. Shao, P. Feng, W. Zuo, H. Wang, Z. Geng, Q. Liu, et al., A novel method for improving the printability of cement-based materials: controlling the releasing of capsules containing chemical admixtures, Cem. Concr. Compos. 128 (2022), 104456, https://doi.org/10.1016/j.cemconcomp.2022.104456.
[2] J.D. Prince, 3D printing: an industrial revolution, J. Electron Resour. Med. Libr 11 (2014) 39–45, https://doi.org/10.1080/15424065.2014.877247.
[3] H. Alghamdi, S.A.O. Nair, N. Neithalath, Insights into material design, extrusion rheology, and properties of 3D-printable alkali-activated fly ash-based binders, Mater. Des. 167 (2019), 107634, https://doi.org/10.1016/j.matdes.2019.107634.
[4] Y. Chen, S.C. Figueiredo, Ç. Yalçinkaya, O. Çopuroğlu, F. Veer, E. Schlangen, The effect of viscosity-modifying admixture on the extrudability of limestone and calcined clay-based cementitious material for extrusion-based 3D concrete printing, Materials 12 (2019) 9–12, https://doi.org/10.3390/ma12091374.
[5] S. Chaves Figueiredo, C. Romero Rodríguez, Z.Y. Ahmed, D.H. Bos, Y. Xu, T.M. Salet, et al., An approach to develop printable strain hardening cementitious composites, Mater. Des. (2019) 169, https://doi.org/10.1016/j.matdes.2019.107651.
[6] V.N. Nerella, M. Näther, A. Iqbal, M. Butler, V. Mechtcherine, Inline quantification of extrudability of cementitious materials for digital construction, Cem. Concr. Compos 95 (2019) 260–270, https://doi.org/10.1016/j.cemconcomp.2018.09.015.
[7] J. Pegna, Exploratory investigation of solid freeform construction, Autom. Constr. 5 (1997) 427–437, https://doi.org/10.1016/S0926-5805(96)00166-5.
[8] T. Wangler, E. Lloret, L. Reiter, N. Hack, F. Gramazio, M. Kohler, et al., Digital concrete: opportunities and challenges, RILEM Tech. Lett. 1 (2016) 67, https://doi.org/10.21809/rilemtechlett.2016.16.
[9] G. De Schutter, K. Lesage, V. Mechtcherine, V.N. Nerella, G. Habert, I. Agusti-Juan, Vision of 3D printing with concrete — Technical, economic and environmental potentials, Cem. Concr. Res 112 (2018) 25–36, https://doi.org/10.1016/j.cemconres.2018.06.001.
[10] M.K. Mohan, A.V. Rahul, G. De Schutter, K. Van Tittelboom, Extrusion-based concrete 3D printing from a material perspective: a state-of-the-art review, Cem. Concr. Compos 115 (2021), 103855, https://doi.org/10.1016/j.cemconcomp.2020.103855.
[11] S. Mindess, Sustainability of Concrete, Elsevier LTD, 2019, https://doi.org/10.1016/B978-0-08-102616-8.00001-0.
[12] I. Agustí-Juan, F. Müller, N. Hack, T. Wangler, G. Habert, Potential benefits of digital fabrication for complex structures: Environmental assessment of a robotically fabricated concrete wall, J. Clean. Prod. 154 (2017) 330–340, https://doi.org/10.1016/j.jclepro.2017.04.002.
[13] Y. Weng, M. Li, S. Ruan, T.N. Wong, M.J. Tan, K.L. Ow Yeong, et al., Comparative economic, environmental and productivity assessment of a concrete bathroom unit fabricated through 3D printing and a precast approach, J. Clean. Prod. 261 (2020), 121245, https://doi.org/10.1016/j.jclepro.2020.121245.
[14] J.G. Sanjayan, B. Nematollahi, M. Xia, T. Marchment, Effect of surface moisture on inter-layer strength of 3D printed concrete, Constr. Build. Mater. 172 (2018) 468–475, https://doi.org/10.1016/j.conbuildmat.2018.03.232.
[15] Y. Han, Z. Yang, T. Ding, J. Xiao, Environmental and economic assessment on 3D printed buildings with recycled concrete, J. Clean. Prod. 278 (2021), 123884, https://doi.org/10.1016/j.jclepro.2020.123884.
[16] A. Cicione, J. Kruger, R.S. Walls, G. Van Zijl, An experimental study of the behavior of 3D printed concrete at elevated temperatures, Fire Saf. J. 120 (2021), 103075, https://doi.org/10.1016/j.firesaf.2020.103075.
[17] Brun F., Gaspar F., Mateus A., Vitorino J., Diz F. Experimental Study on 3D Printing of Concrete with Overhangs. RILEM Int. Conf. Concr. Digit. Fabr., 2020, p. 778–89. https://doi.org/10.1007/978–3-030–49916-7_77.
[18] Z. Liu, M. Li, Y. Weng, T.N. Wong, M.J. Tan, Mixture design approach to optimize the rheological properties of the material used in 3D cementitious material printing, Constr. Build. Mater. 198 (2019) 245–255, https://doi.org/10.1016/j.conbuildmat.2018.11.252.
[19] X. Guo, J. Yang, G. Xiong, Influence of supplementary cementitious materials on rheological properties of 3D printed fly ash based geopolymer, Cem. Concr. Compos. 114 (2020), 103820, https://doi.org/10.1016/j.cemconcomp.2020.103820.
[20] T. Wangler, N. Roussel, F.P. Bos, T.A.M. Salet, R.J. Flatt, Digital concrete: a review, Cem. Concr. Res. (2019) 123, https://doi.org/10.1016/j.cemconres.2019.105780.
[21] D. Dey, D. Srinivas, B. Panda, P. Suraneni, T.G. Sitharam, Use of industrial waste materials for 3D printing of sustainable concrete: a review, J. Clean. Prod. 340 (2022), 130749, https://doi.org/10.1016/j.jclepro.2022.130749.
[22] M. Mazloom, A.A. Ramezanianpour, J.J. Brooks, Effect of silica fume on mechanical properties of high-strength concrete, Cem. Concr. Compos 26 (2004) 347–357, https://doi.org/10.1016/S0958-9465(03)00017-9.
[23] T. Oey, A. Kumar, J.W. Bullard, N. Neithalath, G. Sant, The filler effect: the influence of filler content and surface area on cementitious reaction rates, J. Am. Ceram. Soc. 96 (2013) 1978–1990, https://doi.org/10.1111/jace.12264.
[24] S. Ramanathan, M. Croly, P. Suraneni, Comparison of the effects that supplementary cementitious materials replacement levels have on cementitious paste properties, Cem. Concr. Compos. 112 (2020), 103678, https://doi.org/10.1016/j.cemconcomp.2020.103678.
[25] S. Wild, J.M. Khatib, A. Jones, Relative strength, pozzolanic activity and cement hydration in superplasticised metakaolin concrete, Cem. Concr. Res. 26 (1996) 1537–1544, https://doi.org/10.1016/0008-8846(96)00148-2.
[26] D. Hardjito, S.E. Wallah, D.M.J. Sumajouw, B.V. Rangan, On the development of fly ash-based geopolymer concrete, Acids Mater. J. 101 (2004) 467–472, https://doi.org/10.14359/13485.
[27] D. Hardjito, B.V. Rangan, Development and properties of low-calcium fly ash-based geopolymer concrete, Res Rep. GC (2005) 94.
[28] R. Cyriaque, A. Naghizadeh, L. Tchadjie, A. Adesina, J. Noel, Y. Djobo, et al., Lateritic soils based geopolymer materials: a review, Constr. Build. Mater. 344 (2022), 128157, https://doi.org/10.1016/j.conbuildmat.2022.128157.
[29] A. Gholampour, T. Ozbakkaloglu, C.T. Ng, Ambient- and oven-cured geopolymer concretes under active confinement, Constr. Build. Mater. 228 (2019), 116722, https://doi.org/10.1016/j.conbuildmat.2019.116722.
[30] T. Phoo-Ngernkham, A. Maegawa, N. Mishima, S. Hatanaka, P. Chindaprasirt, Effects of sodium hydroxide and sodium silicate solutions on compressive and shear bond strengths of FA-GBFS geopolymer, Constr. Build. Mater. 91 (2015) 1–8, https://doi.org/10.1016/j.conbuildmat.2015.05.001.

[31] J. Aupoil, J.B. Champenois, J.B. d'Espinose de Lacaillerie, A. Poulesquen, Interplay between silicate and hydroxide ions during geopolymerization, Cem. Concr. Res. 115 (2019) 426–432, https://doi.org/10.1016/j.cemconres.2018.09.012.
[32] R. Vinai, M. Soutsos, Production of sodium silicate powder from waste glass cullet for alkali activation of alternative binders, Cem. Concr. Res. 116 (2019) 45–56, https://doi.org/10.1016/j.cemconres.2018.11.008.
[33] W. Hu, Q. Nie, B. Huang, A. Su, Y. Du, X. Shu, et al., Mechanical property and microstructure characteristics of geopolymer stabilized aggregate base, Constr. Build. Mater. 191 (2018) 1120–1127, https://doi.org/10.1016/j.conbuildmat.2018.10.081.
[34] Q. Nie, W. Hu, T. Ai, B. Huang, X. Shu, Q. He, Strength properties of geopolymers derived from original and desulfurized red mud cured at ambient temperature, Constr. Build. Mater. 125 (2016) 905–911, https://doi.org/10.1016/j.conbuildmat.2016.08.144.
[35] J.S.J. van Deventer, J.L. Provis, P. Duxson, G.C. Lukey, Reaction mechanisms in the geopolymeric conversion of inorganic waste to useful products, J. Hazard Mater. 139 (2007) 506–513, https://doi.org/10.1016/j.jhazmat.2006.02.044.
[36] E. Adesanya, K. Ohenoja, T. Luukkonen, P. Kinnunen, M. Illikainen, One-part geopolymer cement from slag and pretreated paper sludge, J. Clean. Prod. 185 (2018) 168–175, https://doi.org/10.1016/j.jclepro.2018.03.007.
[37] T. Luukkonen, Z. Abdollahnejad, J. Yliniemi, P. Kinnunen, M. Illikainen, Comparison of alkali and silica sources in one-part alkali-activated blast furnace slag mortar, J. Clean. Prod. 187 (2018) 171–179, https://doi.org/10.1016/j.jclepro.2018.03.202.
[38] T. Luukkonen, Z. Abdollahnejad, J. Yliniemi, P. Kinnunen, M. Illikainen, One-part alkali-activated materials: a review, Cem. Concr. Res. 103 (2018) 21–34, https://doi.org/10.1016/j.cemconres.2017.10.001.
[39] H. Zhong, M. Zhang, 3D printing geopolymers: a review, Cem. Concr. Compos. 128 (2022), 104455, https://doi.org/10.1016/j.cemconcomp.2022.104455.
[40] G. Lazorenko, A. Kasprzhitskii, Geopolymer additive manufacturing: a review, Addit. Manuf. 55 (2022), 102782, https://doi.org/10.1016/j.addma.2022.102782.
[41] P. Grassl, H.S. Wong, N.R. Buenfeld, Influence of aggregate size and volume fraction on shrinkage induced micro-cracking of concrete and mortar, Cem. Concr. Res. 40 (2010) 85–93, https://doi.org/10.1016/j.cemconres.2009.09.012.
[42] J. Kruger, S. Zeranka, G. van Zijl, An ab initio approach for thixotropy characterisation of (nanoparticle-infused) 3D printable concrete, Constr. Build. Mater. 224 (2019) 372–386, https://doi.org/10.1016/j.conbuildmat.2019.07.078.
[43] B. Panda, C. Unluer, M.J. Tan, Investigation of the rheology and strength of geopolymer mixtures for extrusion-based 3D printing, Cem. Concr. Compos. 94 (2018) 307–314, https://doi.org/10.1016/j.cemconcomp.2018.10.002.
[44] B. Panda, M.J. Tan, Experimental study on mix proportion and fresh properties of fly ash based geopolymer for 3D concrete printing, Ceram. Int. 44 (2018) 10258–10265, https://doi.org/10.1016/j.ceramint.2018.03.031.
[45] A.V. Rahul, M. Santhanam, H. Meena, Z. Ghani, 3D printable concrete: mixture design and test methods, Cem. Concr. Compos 97 (2019) 13–23, https://doi.org/10.1016/j.cemconcomp.2018.12.014.
[46] M. Nawaz, A. Heitor, M. Sivakumar, Geopolymers in construction - recent developments, Constr. Build. Mater. 260 (2020), 120472, https://doi.org/10.1016/j.conbuildmat.2020.120472.
[47] ASTM C618 - 03. Standard Specification for Coal Fly Ash and Raw or Calcined Natural Pozzolan for Use West Conshohocken, PA, 2001. Annu B ASTM Stand 2010:3–6. https://doi.org/10.1520/C0618–08.
[48] Das S.K., Singh S.K., Mishra J., Mustakim S.M. Effect of Rice Husk Ash and Silica Fume as Strength-Enhancing Materials on Properties of Modern Concrete—A Comprehensive Review BT - Emerging Trends in Civil Engineering. In: Babu KG, Rao HS, Amarnath Y, editors., Singapore: Springer Singapore; 2020, p. 253–66.
[49] Astm C989–04. Standard Specification for Ground Granulated Blast-Furnace Slag for Use in Concrete. Annu B ASTM Stand 2004;i:1–5. https://doi.org/10.1520/C0989–04.
[50] A. Alujas, R. Fernández, R. Quintana, K.L. Scrivener, F. Martirena, Pozzolanic reactivity of low grade kaolinitic clays: Influence of calcination temperature and impact of calcination products on OPC hydration, Appl. Clay Sci. 108 (2015) 94–101, https://doi.org/10.1016/j.clay.2015.01.028.
[51] M. Nodehi, V.M. Taghvaee, Alkali-activated materials and geopolymer: a review of common precursors and activators addressing circular economy, Circ. Econ. Sustain. 2 (2022) 165–196, https://doi.org/10.1007/s43615-021-00029-w.
[52] Provis, J.L., & Van Deventer J.S. Alkali activated materials: state-of-the-art report. 2013. https://doi.org/https://doi.org/10.1007/978–94-007–7672-21.
[53] M. Elzeadani, D.V. Bompa, A.Y. Elghazouli, One part alkali activated materials: a state-of-the-art review Ordinary Portland cement, J. Build. Eng. 57 (2022), 104871, https://doi.org/10.1016/j.jobe.2022.104871.
[54] V. Mechtcherine, V.N. Nerella, F. Will, M. Näther, J. Otto, M. Krause, Large-scale digital concrete construction – CONPrint3D concept for on-site, monolithic 3D-printing, Autom. Constr. 107 (2019), 102933, https://doi.org/10.1016/j.autcon.2019.102933.
[55] S. Lim, R.A. Buswell, T.T. Le, S.A. Austin, A.G.F. Gibb, T. Thorpe, Developments in construction-scale additive manufacturing processes, Autom. Constr. 21 (2012) 262–268, https://doi.org/10.1016/j.autcon.2011.06.010.
[56] M. Xia, B. Nematollahi, J.G. Sanjayan, Development of Powder-Based 3D Concrete Printing Using Geopolymers, Elsevier Inc, 2019, https://doi.org/10.1016/b978-0-12-815481-6.00011-7.
[57] V.N. Nerella, S. Hempel, V. Mechtcherine, Effects of layer-interface properties on mechanical performance of concrete elements produced by extrusion-based 3D-printing, Constr. Build. Mater. 205 (2019) 586–601, https://doi.org/10.1016/j.conbuildmat.2019.01.235.
[58] B. Nematollahi, M. Xia, J. Sanjayan, Post-processing methods to improve strength of particle-bed 3d printed geopolymer for digital construction applications, Front Mater. (2019) 6, https://doi.org/10.3389/fmats.2019.00160.
[59] Khan M.A.. Materials Today: Proceedings Mix suitable for concrete 3D printing: A review. Mater Today Proc 2020;32:831–7. https://doi.org/10.1016/j.matpr.2020.03.825.
[60] M. Chougan, S. Hamidreza Ghaffar, M. Jahanzat, A. Albar, N. Mujaddedi, R. Swash, The influence of nano-additives in strengthening mechanical performance of 3D printed multi-binder geopolymer composites, Constr. Build. Mater. 250 (2020), 118928, https://doi.org/10.1016/j.conbuildmat.2020.118928.
[61] R. Buswell, J. Xu, D. De Becker, J. Dobrzanski, J. Provis, J.T. Kolawole, et al., Geometric quality assurance for 3D concrete printing and hybrid construction manufacturing using a standardised test part for benchmarking capability, Cem. Concr. Res. 156 (2022), 106773, https://doi.org/10.1016/j.cemconres.2022.106773.
[62] D. Lowke, E. Dini, A. Perrot, D. Weger, C. Gehlen, B. Dillenburger, Particle-bed 3D printing in concrete construction – possibilities and challenges, Cem. Concr. Res 112 (2018) 50–65, https://doi.org/10.1016/j.cemconres.2018.05.018.
[63] Jolin M., Burns D., Bissonnette B., Gagnon F., Bolduc L.-S. Understanding the pumpability of concrete. Shotcrete Undergr Support XI Eng Conf Int 2009: 193–207.
[64] F. Bos, R. Wolfs, Z. Ahmed, T. Salet, Additive manufacturing of concrete in construction: potentials and challenges of 3D concrete printing, Virtual Phys. Prototyp. 11 (2016) 209–225, https://doi.org/10.1080/17452759.2016.1209867.
[65] V. Mechtcherine, V.N. Nerella, K. Kasten, Testing pumpability of concrete using Sliding Pipe Rheometer, Constr. Build. Mater. 53 (2014) 312–323, https://doi.org/10.1016/j.conbuildmat.2013.11.037.
[66] S. Muthukrishnan, S. Ramakrishnan, J. Sanjayan, Effect of alkali reactions on the rheology of one-part 3D printable geopolymer concrete, Cem. Concr. Compos. 116 (2021), 103899, https://doi.org/10.1016/j.cemconcomp.2020.103899.
[67] S.F.A. Shah, B. Chen, S.Y. Oderji, M.A. Haque, M.R. Ahmad, Improvement of early strength of fly ash-slag based one-part alkali activated mortar, Constr. Build. Mater. 246 (2020), 118533, https://doi.org/10.1016/j.conbuildmat.2020.118533.
[68] S. Yousefi Oderji, B. Chen, M.R. Ahmad, S.F.A. Shah, Fresh and hardened properties of one-part fly ash-based geopolymer binders cured at room temperature: Effect of slag and alkali activators, J. Clean. Prod. 225 (2019) 1–10, https://doi.org/10.1016/j.jclepro.2019.03.290.
[69] S.H. Bong, B. Nematollahi, M. Xia, A. Nazari, J. Sanjayan, Properties of one-part geopolymer incorporating wollastonite as partial replacement of geopolymer precursor or sand, Mater. Lett. 263 (2020), 127236, https://doi.org/10.1016/j.matlet.2019.127236.

[70] S.H. Bong, B. Nematollahi, M. Xia, S.H. Ghaffar, J. Pan, J.G. Dai, Properties of additively manufactured geopolymer incorporating mineral wollastonite microfibers, Constr. Build. Mater. 331 (2022), 127282, https://doi.org/10.1016/j.conbuildmat.2022.127282.
[71] N. Roussel, Rheological requirements for printable concretes, Cem. Concr. Res. 112 (2018) 76–85, https://doi.org/10.1016/j.cemconres.2018.04.005.
[72] B. Felekoğlu, S. Türkel, B. Baradan, Effect of water/cement ratio on the fresh and hardened properties of self-compacting concrete, Build. Environ. 42 (2007) 1795–1802, https://doi.org/10.1016/j.buildenv.2006.01.012.
[73] Y. Cheng, P. Cong, H. Hao, Q. Zhao, L. Mei, A. Zhang, et al., Improving workability and mechanical properties of one-part waste brick power based-binders with superplasticizers, Constr. Build. Mater. 335 (2022), 127535, https://doi.org/10.1016/j.conbuildmat.2022.127535.
[74] Y. Alrefaei, Y.S. Wang, J.G. Dai, Q.F. Xu, Effect of superplasticizers on properties of one-part Ca(OH)2/Na2SO4 activated geopolymer pastes, Constr. Build. Mater. 241 (2020), 117990, https://doi.org/10.1016/j.conbuildmat.2019.117990.
[75] A. Kazemian, X. Yuan, E. Cochran, B. Khoshnevis, Cementitious materials for construction-scale 3D printing: laboratory testing of fresh printing mixture, Constr. Build. Mater. 145 (2017) 639–647, https://doi.org/10.1016/j.conbuildmat.2017.04.015.
[76] S.H. Bong, B. Nematollahi, A. Nazari, M. Xia, J. Sanjayan, Efficiency of different superplasticizers and retarders on properties of "one-part" fly ash-slag blended geopolymers with different activators, Materials (2019) 12, https://doi.org/10.3390/ma12203410.
[77] S.H. Bong, M. Xia, B. Nematollahi, C. Shi, Ambient temperature cured 'just-add-water' geopolymer for 3D concrete printing applications, Cem. Concr. Compos 121 (2021), 104060, https://doi.org/10.1016/j.cemconcomp.2021.104060.
[78] M. Chougan, S.H. Ghaffar, P. Sikora, S.Y. Chung, T. Rucinska, D. Stephan, et al., Investigation of additive incorporation on rheological, microstructural and mechanical properties of 3D printable alkali-activated materials, Mater. Des. (2021) 202, https://doi.org/10.1016/j.matdes.2021.109574.
[79] B. Panda, G.B. Singh, C. Unluer, M.J. Tan, Synthesis and characterization of one-part geopolymers for extrusion based 3D concrete printing, J. Clean. Prod. 220 (2019) 610–619, https://doi.org/10.1016/j.jclepro.2019.02.185.
[80] Z. Abdollahnejad, T. Luukkonen, M. Mastali, C. Giosue, O. Favoni, M.L. Ruello, et al., Microstructural analysis and strength development of one-part alkali-activated slag/ceramic binders under different curing regimes, Waste Biomass. Valoriz. 11 (2020) 3081–3096, https://doi.org/10.1007/s12649-019-00626-9.
[81] G. Ma, Y. Yan, M. Zhang, J. Sanjayan, Effect of steel slag on 3D concrete printing of geopolymer with quaternary binders, Ceram. Int (2022), https://doi.org/10.1016/j.ceramint.2022.05.305.
[82] B. Panda, S. Ruan, C. Unluer, M.J. Tan, Investigation of the properties of alkali-activated slag mixes involving the use of nanoclay and nucleation seeds for 3D printing, Compos. Part B Eng. 186 (2020), 107826, https://doi.org/10.1016/j.compositesb.2020.107826.
[83] T. Yang, X. Gao, J. Zhang, X. Zhuang, H. Wang, Z. Zhang, Sulphate resistance of one-part geopolymer synthesized by calcium carbide residue-sodium carbonate-activation of slag, Compos. Part B 242 (2022), 110024, https://doi.org/10.1016/j.compositesb.2022.110024.
[84] X. Gao, X. Yao, T. Yang, S. Zhou, H. Wei, Z. Zhang, Calcium carbide residue as auxiliary activator for one-part sodium carbonate-activated slag cements: compressive strength, phase assemblage and environmental benefits, Constr. Build. Mater. 308 (2021), 125015, https://doi.org/10.1016/j.conbuildmat.2021.125015.
[85] T. Yang, Z. Zhang, F. Zhang, Y. Gao, Q. Wu, Chloride and heavy metal binding capacities of hydrotalcite-like phases formed in greener one-part sodium carbonate-activated slag cements, J. Clean. Prod. 253 (2020), 120047, https://doi.org/10.1016/j.jclepro.2020.120047.
[86] C. Shi, B. Qu, J.L. Provis, Recent progress in low-carbon binders, Cem. Concr. Res 122 (2019) 227–250, https://doi.org/10.1016/j.cemconres.2019.05.009.
[87] S. Pangdaeng, T. Phoo-ngernkham, V. Sata, P. Chindaprasirt, Influence of curing conditions on properties of high calcium fly ash geopolymer containing Portland cement as additive, Mater. Des. 53 (2014) 269–274, https://doi.org/10.1016/j.matdes.2013.07.018.
[88] C. Zhang, V.N. Nerella, A. Krishna, S. Wang, Y. Zhang, V. Mechtcherine, et al., Mix design concepts for 3D printable concrete: a review, Cem. Concr. Compos 122 (2021), 104155, https://doi.org/10.1016/j.cemconcomp.2021.104155.
[89] C. Lu, Z. Zhang, C. Shi, N. Li, D. Jiao, Q. Yuan, Rheology of alkali-activated materials: a review, Cem. Concr. Compos 121 (2021), 104061, https://doi.org/10.1016/j.cemconcomp.2021.104061.
[90] N. Roussel, A thixotropy model for fresh fluid concretes: theory, validation and applications, Cem. Concr. Res 36 (2006) 1797–1806, https://doi.org/10.1016/j.cemconres.2006.05.025.
[91] Rodrigue C., Lecomte-nana L., Adesina A. Influence of mineralogy and activator type on the rheology behaviour and setting time of laterite based geopolymer paste 2022;126. https://doi.org/10.1016/j.cemconcomp.2021.104345.
[92] C.R. Kaze, T. Alomayri, A. Hasan, S. Tome, G.L. Lecomte-Nana, J.G.D. Nemaleu, et al., Reaction kinetics and rheological behaviour of meta-halloysite based geopolymer cured at room temperature: effect of thermal activation on physicochemical and microstructural properties, Appl. Clay Sci. 196 (2020), 105773, https://doi.org/10.1016/j.clay.2020.105773.
[93] C. Rodrigue, A. Adesina, T. Alomayri, H. Assaedi, E. Kamseu, U. Chinje, et al., Characterization, reactivity and rheological behaviour of metakaolin and Meta-halloysite based geopolymer binders, Clean. Mater. 2 (2021), 100025, https://doi.org/10.1016/j.clema.2021.100025.
[94] C.R. Kaze, A. Adesina, G.L. Lecomte-Nana, T. Alomayri, E. Kamseu, U.C. Melo, Alkali-activated laterite binders: Influence of silica modulus on setting time, rheological behaviour and strength development, Clean. Eng. Technol. (2021) 4, https://doi.org/10.1016/j.clet.2021.100175.
[95] V. Mechtcherine, F.P. Bos, A. Perrot, W.R.L. da Silva, V.N. Nerella, S. Fataei, et al., Extrusion-based additive manufacturing with cement-based materials – Production steps, processes, and their underlying physics: a review, Cem. Concr. Res. 132 (2020), 106037, https://doi.org/10.1016/j.cemconres.2020.106037.
[96] J. Xie, J. Wang, R. Rao, C. Wang, C. Fang, Effects of combined usage of GGBS and fly ash on workability and mechanical properties of alkali activated geopolymer concrete with recycled aggregate, Compos. Part B Eng. 164 (2019) 179–190, https://doi.org/10.1016/j.compositesb.2018.11.067.
[97] M. Dong, M. Elchalakani, A. Karrech, Development of high strength one-part geopolymer mortar using sodium metasilicate, Constr. Build. Mater. 236 (2020), 117611, https://doi.org/10.1016/j.conbuildmat.2019.117611.
[98] C. Ma, B. Zhao, S. Guo, G. Long, Y. Xie, Properties and characterization of green one-part geopolymer activated by composite activators, J. Clean. Prod. 220 (2019) 188–199, https://doi.org/10.1016/j.jclepro.2019.02.159.
[99] C. Sun, J. Xiang, M. Xu, Y. He, Z. Tong, X. Cui, 3D extrusion free forming of geopolymer composites: materials modification and processing optimization, J. Clean. Prod. 258 (2020), 120986, https://doi.org/10.1016/j.jclepro.2020.120986.
[100] Z. Abdollahnejad, T. Luukkonen, M. Mastali, P. Kinnunen, M. Illikainen, Development of one-part alkali-activated ceramic/slag binders containing recycled ceramic aggregates, J. Mater. Civ. Eng. 31 (2019) 1–13, https://doi.org/10.1061/(asce)mt.1943-5533.0002608.
[101] P. Nuaklong, V. Sata, P. Chindaprasirt, Properties of metakaolin-high calcium fly ash geopolymer concrete containing recycled aggregate from crushed concrete specimens, Constr. Build. Mater. 161 (2018) 365–373, https://doi.org/10.1016/j.conbuildmat.2017.11.152.
[102] Z. Chen, Z. Li, J. Li, C. Liu, C. Lao, Y. Fu, et al., 3D printing of ceramics: a review, J. Eur. Ceram. Soc. 39 (2019) 661–687, https://doi.org/10.1016/j.jeurceramsoc.2018.11.013.
[103] B. Panda, S. Chandra Paul, M. Jen Tan, Anisotropic mechanical performance of 3D printed fiber reinforced sustainable construction material, Mater. Lett. 209 (2017) 146–149, https://doi.org/10.1016/j.matlet.2017.07.123.
[104] A.V. Rahul, M. Santhanam, H. Meena, Z. Ghani, Mechanical characterization of 3D printable concrete, Constr. Build. Mater. 227 (2019), 116710, https://doi.org/10.1016/j.conbuildmat.2019.116710.
[105] S. Guo, C. Ma, G. Long, Y. Xie, Cleaner one-part geopolymer prepared by introducing fly ash sinking spherical beads: properties and geopolymerization mechanism, J. Clean. Prod. 219 (2019) 686–697, https://doi.org/10.1016/j.jclepro.2019.02.116.
[106] A.R. Arunothayan, B. Nematollahi, R. Ranade, S.H. Bong, J. Sanjayan, Development of 3D-printable ultra-high performance fiber-reinforced concrete for digital construction, Constr. Build. Mater. 257 (2020), 119546, https://doi.org/10.1016/j.conbuildmat.2020.119546.
[107] Y. Chen, L. Jia, C. Liu, Z. Zhang, L. Ma, C. Chen, et al., Mechanical anisotropy evolution of 3D-printed alkali-activated materials with different GGBFS/FA combinations, J. Build. Eng. 50 (2022), 104126, https://doi.org/10.1016/j.jobe.2022.104126.
[108] J. Xiao, H. Liu, T. Ding, Finite element analysis on the anisotropic behavior of 3D printed concrete under compression and flexure, Addit. Manuf. 39 (2021), 101712, https://doi.org/10.1016/j.addma.2020.101712.

[109] T. Ding, J. Xiao, S. Zou, J. Yu, Flexural properties of 3D printed fiber-reinforced concrete with recycled sand, Constr. Build. Mater. 288 (2021), 123077, https://doi.org/10.1016/j.conbuildmat.2021.123077.
[110] M. Batikha, R. Jotangia, M.Y. Baaj, I. Mousleh, 3D concrete printing for sustainable and economical construction: a comparative study, Autom. Constr. 134 (2022), 104087, https://doi.org/10.1016/j.autcon.2021.104087.
[111] B. García de Soto, I. Agustí-Juan, J. Hunhevicz, S. Joss, K. Graser, G. Habert, et al., Productivity of digital fabrication in construction: cost and time analysis of a robotically built wall, Autom. Constr. 92 (2018) 297–311, https://doi.org/10.1016/j.autcon.2018.04.004.
[112] B. Panda, S.C. Paul, L.J. Hui, Y.W.D. Tay, M.J. Tan, Additive manufacturing of geopolymer for sustainable built environment, J. Clean. Prod. 167 (2017) 281–288, https://doi.org/10.1016/j.jclepro.2017.08.165.
[113] B.C. McLellan, R.P. Williams, J. Lay, A. Van Riessen, G.D. Corder, Costs and carbon emissions for geopolymer pastes in comparison to ordinary portland cement, J. Clean. Prod. 19 (2011) 1080–1090, https://doi.org/10.1016/j.jclepro.2011.02.010.
[114] R. Abbas, M.A. Khereby, H.Y. Ghorab, N. Elkhoshkhany, Preparation of geopolymer concrete using Egyptian kaolin clay and the study of its environmental effects and economic cost, Clean. Technol. Environ. Policy 22 (2020) 669–687, https://doi.org/10.1007/s10098-020-01811-4.
[115] K.H. Yang, K.H. Lee, J.K. Song, M.H. Gong, Properties and sustainability of alkali-activated slag foamed concrete, J. Clean. Prod. 68 (2014) 226–233, https://doi.org/10.1016/j.jclepro.2013.12.068.
[116] C. Ma, G. Long, Y. Shi, Y. Xie, Preparation of cleaner one-part geopolymer by investigating different types of commercial sodium metasilicate in China, J. Clean. Prod. 201 (2018) 636–647, https://doi.org/10.1016/j.jclepro.2018.08.060.
[117] G. Habert, C. Ouellet-Plamondon, Recent update on the environmental impact of geopolymers, RILEM Tech. Lett. 1 (2016) 17, https://doi.org/10.21809/rilemtechlett.v1.6.
[118] M. Mohammad, E. Masad, S.G. Al-Ghamdi, 3D concrete printing sustainability: a comparative life cycle assessment of four construction method scenarios, Buildings 10 (2020) 245, https://doi.org/10.3390/buildings10120245.
[119] M.K. Mohan, A.V. Rahul, K. Van Tittelboom, G. De Schutter, Rheological and pumping behaviour of 3D printable cementitious materials with varying aggregate content, Cem. Concr. Res 139 (2021), 106258, https://doi.org/10.1016/j.cemconres.2020.106258.
[120] L. Barcelo, J. Kline, G. Walenta, E. Gartner, Cement and carbon emissions, Mater. Struct. Constr. 47 (2014) 1055–1065, https://doi.org/10.1617/s11527-013-0114-5.
[121] Y. Yao, M. Hu, F. Di Maio, S. Cucurachi, Life cycle assessment of 3D printing geo-polymer concrete: an ex-ante study, J. Ind. Ecol. 24 (2020) 116–127, https://doi.org/10.1111/jiec.12930.
[122] S. Liu, B. Lu, H. Li, Z. Pan, J. Jiang, S. Qian, A comparative study on environmental performance of 3D printing and conventional casting of concrete products with industrial wastes, Chemosphere (2022) 298, https://doi.org/10.1016/j.chemosphere.2022.134310.
[123] S.Y. Kwek, H. Awang, C.B. Cheah, Influence of liquid-to-solid and alkaline activator (Sodium silicate to sodium hydroxide) ratios on fresh and hardened properties of alkali-activated palm oil fuel ash geopolymer, Materials (2021) 14, https://doi.org/10.3390/ma14154253.
[124] L.K. Turner, F.G. Collins, Carbon dioxide equivalent (CO_2-e) emissions: a comparison between geopolymer and OPC cement concrete, Constr. Build. Mater. 43 (2013) 125–130, https://doi.org/10.1016/j.conbuildmat.2013.01.023.
[125] A. Petrillo, R. Cioffi, C. Ferone, F. Colangelo, C. Borrelli, Eco-sustainable geopolymer concrete blocks production process, Agric. Agric. Sci. Procedia 8 (2016) 408–418, https://doi.org/10.1016/j.aaspro.2016.02.037.
[126] S.C. Paul, Y.W.D. Tay, B. Panda, M.J. Tan, Fresh and hardened properties of 3D printable cementitious materials for building and construction, Arch. Civ. Mech. Eng. 18 (2018) 311–319, https://doi.org/10.1016/j.acme.2017.02.008.
[127] CEMBUREAU. Activity Report 2020, CEMBUREAU: The European Association 2020. https://cembureau.eu/media/1sjf4sk4/cembureau-activity-report-2020.pdf (accessed August 1, 2022).